Resonance of the magnetophonon conductivity in two-dimensional systems

C. E. Leal and I. C. da Cunha Lima
Instituto de Pesquisas Espaciais (INPE), avenida dos Astronautas 1758, Caixa Postal 515, 12 201 São José Campos, São Paulo, Brazil

A. Troper
Centro Brasileiro de Pesquisas Físicas (CBPF), rua Xavier Sigaud 150, 22 290 Rio de Janeiro, Rio de Janiero, Brazil
(Received 27 October 1989)

In this work, we have investigated the behavior of the line shape of the cyclotron resonance for a two-dimensional electron gas interacting with longitudinal-surface-acoustical phonons, in the presence of a strong magnetic field. The magnetophonon conductivity is evaluated in terms of the dissipative and reactive effects on the electron gas, using the memory-function formalism. New results for both temperature and magnetic field dependences of the cyclotron resonance are studied and compared with conflicting points of previous works. Besides, it is shown that a splitting on the dynamical conductivity peak should always be expected for magnetic fields lower than the corresponding one to the quantum limit, i.e., with only the first Landau level occupied, in agreement with what has been found experimentally.

I. INTRODUCTION

In recent years there has been much interest in the magnetotransport properties of a two-dimensional electron gas (2D EG) confined to a plane as in the silicon metal-oxide-semiconductor field-effect transistor (MOSFET) or in $Ga_{1-x}Al_xAs/GaAs$ heterostructures.[1] The cyclotron resonance (CR) in a high magnetic field applied in the direction normal to the electron layer has been one of the most useful tools for investigating the dynamical properties of such materials, for various scattering mechanisms.[1,2] For instance, the CR measurements obtained from a magneto-optical absorption spectrum of a 2D EG interacting with longitudinal-optical (LO) phonons can give important descriptions of polaronic effects, e.g., the polaron cyclotron resonance mass renormalization.[3]

In a general form, the interaction between the 2D EG and bulk LO phonons as well as 3D longitudinal acoustical (LA) phonons have been the subject of a great number of theoretical[3-5] and experimental studies.[6,7] On the other hand, a small number of theoretical works exist aiming to investigate the role of the interaction between two-dimensional electrons and surface-phonon modes.[8,9] In Ref. 9, the authors showed that the dominant contribution of the electron-phonon interaction, in the case of thin quantum wells, arises mainly from the interface modes, whereas the largest contribution for thick layers larger than 100 Å comes out of the bulk phonon modes. Furthermore, recent experimental data revealed some interesting aspects of this kind of scattering process. For instance, the work of Wixforth *et al.*[6] showed that for some heterostructure architectures, the 2D electron –surface-acoustic-phonon interaction under strong magnetic field may be responsible for quantum oscillations in the sound attenuation. Also, Brumell *et al.*[7] suggested that the observed temperature behavior of the magnetophonon resonance on $Ga_{1-x}Al_xAs/GaAs$ heterostructure could arise from the scattering of the 2D EG by interface LO phonons.

In this sense we are interested in describing the fundamental role of the electron- and surface-phonon interaction in a 2D EG for studies of the cyclotron resonance. The properties of the CR of the two-dimensional electron gas interacting with LA phonons were first studied by Horovitz *et al.*[5] and more recently by Hu and O'Connell.[10] Meanwhile, some fundamental aspects on the electron dynamics, which were not considered in previous works, are described here in a systematic way. The electron-phonon interaction is treated here in terms of the memory-function (MF) formalism for the case of LA phonon scattering. We evaluated the dynamic transport properties of a 2D EG, within a simple model for finite temperature, discussing the electron-phonon scattering in terms of the bare density-density correlation function, at low-density limit, in such a way that screening effects may be neglected. Furthermore, the broadening of the Landau levels, due to impurity scattering,[1] as much as the nonparabolicity effect of the conduction band[3] are also neglected for the sake of simplicity. In Sec. II we present the memory-function approach. A systematic analysis of the temperature and magnetic field behavior of the MF contributions is performed in Sec. III together with the numerical calculation of the magnetoconductivity. Finally, in Sec. IV we summarize the main conclusions and make supplementary comments concerning some controversial points with previous works.

II. MODEL HAMILTONIAN AND MEMORY-FUNCTION FORMALISM

It is well known that when a strong magnetic field **H** is applied perpendicular to the 2D electron motion, such as formed in inversion layers in MOSFET or other semiconductor heterostructures, the energy levels of the 2D

noninteracting electron gas are completely quantized into discrete Landau levels. In the absence of impurity scatterers, the 2D density of states becomes a collection of Dirac δ functions at the positions of each Landau level. In this sense, neglecting impurity scattering, we will treat here only the interaction between the 2D EG and the surface LA phonons, under the action of a perpendicular high magnetic field. The Hamiltonian describing this interaction is given by

$$H=\sum_{n,\mathbf{k}}\hbar\omega_c(n+\tfrac{1}{2})C^{\dagger}_{n,\mathbf{k}}C_{n,\mathbf{k}}+\sum_{\mathbf{q}}\hbar\omega_q b^{\dagger}_{\mathbf{q}}b_{\mathbf{q}} + \sum_{n,\mathbf{q}}D(\mathbf{q})e^{i\mathbf{q}\cdot\mathbf{r}}(b_{\mathbf{q}}+b^{\dagger}_{-\mathbf{q}}) , \tag{1}$$

where the first term represents Landau quasiparticles with energy ε_n, with $n=0,1,2,\ldots$ being the Landau-level index. The frequency $\omega_c=eH/m_b$ is the bare cyclotron frequency, whereas m_b means the effective band mass. In the above equation, ω_q is the 2D LA-phonon frequency, whereas $b_{\mathbf{q}}$ and $b^{\dagger}_{\mathbf{q}}$ are the destruction and creation phonon operators and $D(\mathbf{q})$ is the electron-phonon interaction potential. Moreover, all vectors appearing in the above equation are 2D vectors in the X-Y plane.

In the holomorphic memory-function approach of Götze and Wölfle,[11] the dynamical conductivity at finite magnetic field can be expressed as[12]

$$\sigma_{\pm}(\omega)=\sigma_{xx}(\omega)\pm i\sigma_{xy}(\omega)=\frac{in_e e^2}{m_b}[\omega\mp\omega_c+M(\omega)]^{-1} , \tag{2}$$

with

$$M(\omega)=M_1(\omega)+iM_2(\omega) , \tag{3}$$

where $\sigma_{xx}(\omega)$ and $\sigma_{xy}(\omega)$ are the two-dimensional transverse and Hall conductivities, respectively, whereas $+$ $(-)$ denotes the left (right) circularly polarized wave and n_e means the total number of carriers per unit area with charge $-|e|$. $M_1(\omega)$ and $M_2(\omega)$ are the real and the imaginary diagonal parts of the so-called memory function, $M(\omega)$.[13] They describe, respectively, the reactive and the dissipative effects on the electron dynamics, and are responsible for the shift and the width of the cyclotron resonance line.

In our derivations, we express the memory function in terms of the diagonal (retarded) force-force correlation function, $\Pi^R_{xx}(\omega)$. Using the projection-operator formalism,[14] one gets

$$M_{xx}(\omega)=-\frac{1}{n_e m_b\omega}[\Pi^R_{xx}(\omega)-\Pi^R_{xx}(0)] , \tag{4}$$

where

$$\Pi^R_{xx}(\omega)=-2\sum_{n,n',\mathbf{q}}q_x^2|D(\mathbf{q})|^2\left[\left[\frac{\eta_F(\varepsilon_n)-\eta_F(\varepsilon_{n'})}{\omega+\omega_{n,n'}-\omega_q}C_{n,n'}(q)[\eta_B(\omega_q)-\eta_B(\omega_{n,n'})]\right]-(\omega_q\rightarrow-\omega_q)\right] . \tag{5}$$

In the above equation the terms $\eta_F(\varepsilon)$ and $\eta_B(\omega)$ denote, respectively, the Fermi-Dirac and Bose-Einstein distribution functions. The double summation over the Landau-level indices n and n' reflects the possibility of transitions between different states, with the energy separation given by

$$\omega_{n,n'}=(\varepsilon_{n'}-\varepsilon_n)=(n'-n)\hbar\omega_c . \tag{6}$$

The function $C_{n,n'}(q)$ (Ref. 12) appearing in Eq. (5) is given by

$$C_{n,n'}(q)=\frac{1}{2\pi l_0^2}\frac{n!}{n'!}\left[\frac{l_0 q}{\sqrt{2}}\right]^{2(n'-n)}e^{-l_0^2q^2/2}[L_n^{n'-n}(l_0^2q^2/2)]^2 , \tag{7}$$

where $L_n^{n'-n}(x)$ is the generalized Laguerre polynomial[15] and $l_0=(\hbar/m_b\omega_c)^{1/2}$ stands for the magnetic radius length. In the Bohm-Pines random-phase approximation, the polarization function for noninteracting 2D electron gas is

$$\chi(\mathbf{q},\omega)=\sum_{n,n'}\chi_{n,n'}(\mathbf{q},\omega)=\sum_{n,n'}\frac{[\eta_F(\varepsilon_n)-\eta_F(\varepsilon_{n'})]}{\omega+\omega_{n,n'}+i\delta}C_{n,n'}(q) , \tag{8}$$

with

$$\chi(\mathbf{q},\omega)=\sum_{n,n'}\chi'_{n,n'}(\mathbf{q},\omega)+i\chi''_{n,n'}(\mathbf{q},\omega) . \tag{9}$$

The real and imaginary parts of the MF which are related to each other by the Kramers-Kronig relation can be written, after some algebra, in terms of the polarization function as

$$M_2(\omega)=\frac{-2}{n_e m_b\omega}\sum_{\mathbf{q}}q_x^2|D(\mathbf{q})|^2\{[\eta_B(\omega_q)-\eta_B(\omega+\omega_q)]\chi''(\mathbf{q},\omega+\omega_q)+[\eta_B(\omega_q)-\eta_B(\omega_q-\omega)]\chi''(\mathbf{q},\omega-\omega_q)\} , \tag{10}$$

and

$$M_1(\omega)=\frac{2}{n_e m_b \omega}\sum_{\mathbf{q}} q_x^2|D(\mathbf{q})|^2\left\{\coth(\beta\omega_q/2)[\chi'(\mathbf{q},\omega+\omega_q)+\chi'(\mathbf{q},\omega-\omega_q)-2\chi'(\mathbf{q},\omega_q)]\right.$$
$$\left.+\sum_{n,n'}\coth(\beta\omega_{n,n'}/2)[\chi'_{n,n'}(\mathbf{q},\omega+\omega_q)+\chi'_{n,n'}(\mathbf{q},\omega-\omega_q)-2\chi'_{n,n'}(\mathbf{q},\omega_q)]\right\}, \tag{11}$$

with $\beta=(k_B T)^{-1}$, where k_B is the Boltzmann constant and T is the temperature. The factor 2 in the above equations arises from the spin index summation. Thus, according to Eqs. (2) and (3) we obtain directly the real and imaginary part of the dynamical conductivity $\sigma_{\pm}(\omega)$ as

$$\mathrm{Re}\sigma_{\pm}(\omega)=\frac{n_e e^2}{m_b}\frac{M_2(\omega)}{[\omega\mp\omega_c+M_1(\omega)]^2+[M_2(\omega)]^2}, \tag{12}$$

and

$$\mathrm{Im}\sigma_{\pm}(\omega)=\frac{n_e e^2}{m_b}\frac{\omega\mp\omega_c+M_1(\omega)}{[\omega\mp\omega_c+M_1(\omega)]^2+[M_2(\omega)]^2}. \tag{13}$$

III. EVALUATION OF THE MF CONTRIBUTIONS AND NUMERICAL RESULTS

In this section we perform the evaluation of the frequency-dependent MF, as a function of the temperature and the magnetic field. We describe the 2D electron–LA-phonon interaction in terms of the deformation potential matrix element $D_{\mathrm{LA}}(\mathbf{q})$ (Ref. 16) and the Debye model for the phonon frequency, i.e., $\omega_q=c_s q$, with c_s being the velocity of the surface acoustic waves. In the case of Si MOSFET,[17]

$$D_{\mathrm{LA}}(\mathbf{q})=\frac{\hbar\Xi_d^2 q^2}{2\rho\omega_q d}, \tag{14}$$

where Ξ_d means the deformation potential coupling, ρ is the mass density, and d is the thickness of the inversion layer.

Then, performing the substitutions in Eq. (10), we find

$$M_2(\omega)=\frac{\hbar\pi l_0^3\alpha}{8m_b^2}\sum_{n,n'}\int_0^{\infty}dq\,q^4\frac{1}{(1-e^{-\hbar\beta\omega_q})}C_{n,n'}(q)[\eta_F(\varepsilon_n)-\eta_F(\varepsilon_{n'})]$$
$$\times\left\{\left[\frac{(\omega)^{-1}e^{\hbar\beta\omega}}{(e^{\hbar\beta(\omega+\omega_q)}-1)}\delta(\hbar\omega+\hbar\omega_q-\omega_{n,n'})\right]+(\omega\rightarrow-\omega)\right\}, \tag{15}$$

where

$$\alpha=\frac{2\Xi_d^2 m_b}{n_e\rho d c_s\pi l_0^3}. \tag{16}$$

In the present approach, no overlap of the density of states of the adjacent Landau levels is considered and only transitions between Landau levels, due to thermal electron excitations, are responsible for the electron dynamics. It is requested that the available transition contributions must satisfy the conditions $0\le n\le(N_{\max}-1)$ and $n'>(N_{\max}-1)$, where $N_{\max}$ means the maximum number of levels completely filled. On the other hand, there are some prohibited transitions, since we assume that the Landau levels are either fully occupied or empty, and then the Fermi level E_F lies midway between the last occupied Landau level and the first unoccupied one.

Then, we can write $M_2(\omega)$ in the following way:

$$M_2(\omega)=\frac{\hbar\pi l_0^3\alpha}{8m_b^2}\int_0^{\infty}dq\,q^4\frac{1}{(1-e^{-\hbar\beta\omega_q})}\sum_{n,m}C_{n,n+m}(q)\Theta(E_F-\varepsilon_n)\Theta(\varepsilon_{n+m}-E_F)$$
$$\times\left\{(\omega)^{-1}\frac{(e^{\hbar\beta\omega}-1)}{(e^{\hbar\beta(\omega_q+\omega)}-1)}\delta(\hbar\omega_q-m\hbar\omega_c+\hbar\omega)\right.$$
$$+(-\omega)^{-1}\frac{(e^{-\hbar\beta\omega}-1)}{(e^{\hbar\beta(\omega_q-\omega)}-1)}[\delta(\hbar\omega_q-m\hbar\omega_c-\hbar\omega)$$
$$\left.-\delta(\hbar\omega_q+m\hbar\omega_c-\hbar\omega)]\right\}, \tag{17}$$

with n' being replaced by $n+m$, where m is a positive integer ($m=1,2,3,\ldots$). $\Theta(x)$ is the Heaviside step function, so

that $\Theta(x)=1$ if $x>0$ and $\Theta(x)=0$ if $x<0$.

Finally, evaluating all terms in the above equation, we obtain, for the imaginary MF,

$$M_2(y)=\frac{\pi l_0^7\omega_c^5\alpha}{8y\hbar^2c_s^5}\sum_{n,m}\Theta(E_F-\varepsilon_n)\Theta(\varepsilon_{n+m}-E_F)$$
$$\times\left[(m-y)^4\frac{1}{(1-e^{-\hbar\beta\omega_c(m-y)})}\frac{(e^{y\hbar\beta\omega_c}-1)}{(e^{m\hbar\beta\omega_c}-1)}C_{n,n+m}((m-y)\omega_c/c_s)\Theta(m-y)\right.$$
$$+(y-m)^4\frac{1}{(1-e^{-\hbar\beta\omega_c(y-m)})}\frac{(e^{-y\hbar\beta\omega_c}-1)}{(e^{-m\hbar\beta\omega_c}-1)}C_{n,n+m}((y-m)\omega_c/c_s)\Theta(y-m)$$
$$\left.-(m+y)^4\frac{1}{(1-e^{-\hbar\beta\omega_c(m+y)})}\frac{(e^{-y\hbar\beta\omega_c}-1)}{(e^{m\hbar\beta\omega_c}-1)}C_{n,n+m}((m+y)\omega_c/c_s)\right], \tag{18}$$

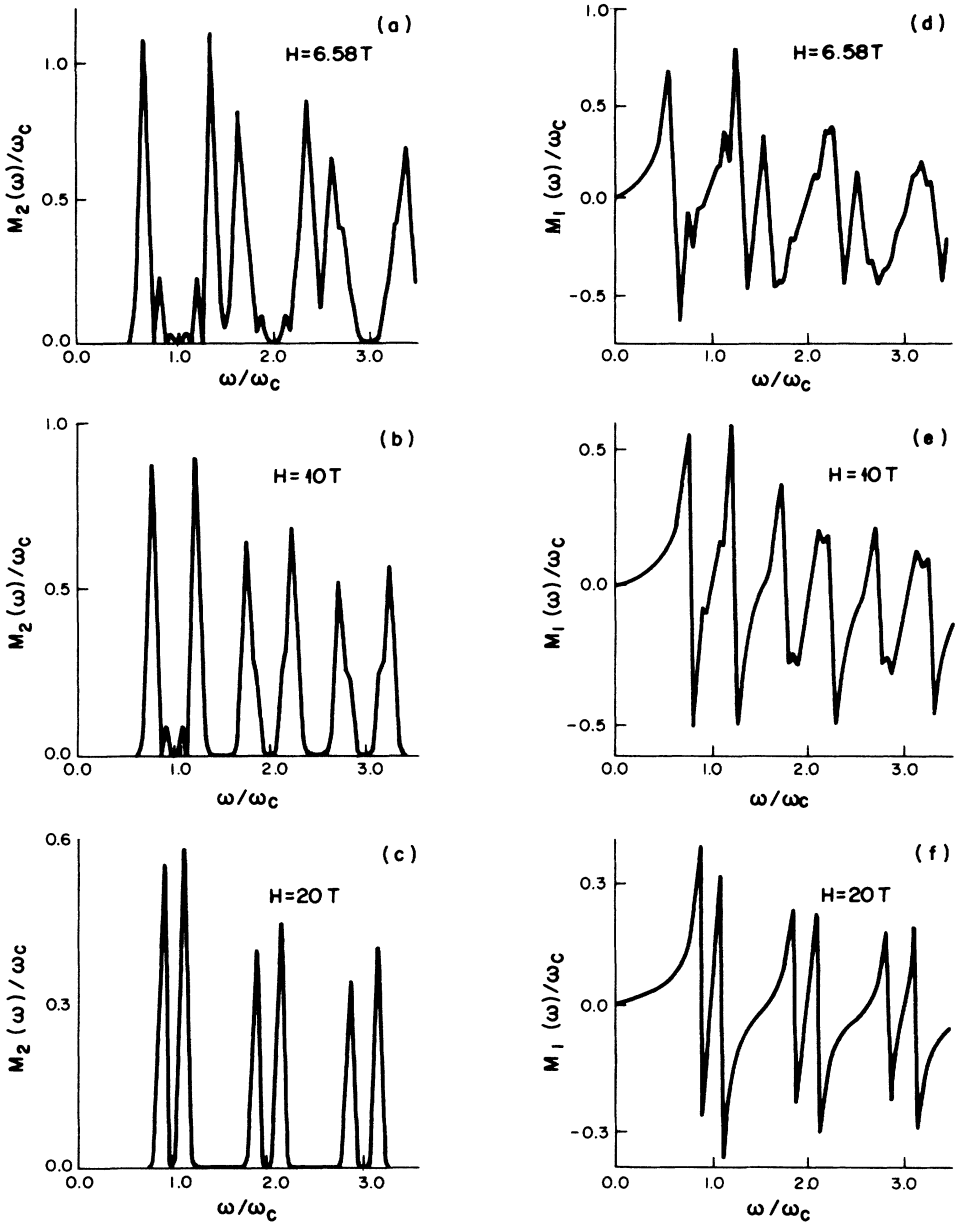

FIG. 1. Frequency behavior of $M_2(w)$ and $M_1(w)$, in units of w_c, exhibited for different values of the magnetic fields.

where we have introduced the dimensionless quantity y, defined as $y=\omega/\omega_c$.

On the above equation the first and the second terms correspond, respectively, to phonon absorption ($m>y$) and phonon emission ($y>m$). Our numerical results have revealed that the last term in Eq. (18) arising from emission of phonons with large wave vector is very small. This shows that the main contribution in this kind of interaction is basically due to scattering by phonons with small wave vector.[5] According to Eq. (18) it is easy to verify that $M_2(w)$ has a linear temperature dependence, for both low- and high-temperature limits, in good agreement with experimental data.[18] A similar result for the imaginary MF part was obtained previously in Ref. 10. However, it must be emphasized that some physical aspects of the 2D EG under the action of a magnetic field were not taken into account by those authors, e.g., the existence of some unallowed transitions. Besides, we have verified that each allowed transition associated with an initial occupied state n ($n>0$) gives rise to n dips of $M_2(w)$, in addition to those which occur at y integer and half-integer (Fig. 3). This as a direct result of the number of roots of the corresponding Laguerre polinomial, $L_n^m(x)$,[15] in Eq. (7). Consequently, since the number of filled Landau levels in the system increases as the intensity of the magnetic field decreases, a more complex structure of the MF is expected for the case of lower magnetic fields in contrast to a singular structure in the quantum limit case, as can be seen in Fig. 1.

Now we may use the Kramers-Kronig relation in order to calculate the expression of the real MF part,

$$M_1(w)=2\frac{w}{\pi}\mathrm{P}\int_0^\infty dw'\frac{M_2(w')}{(w')^2-w^2}\ , \tag{19}$$

where P stands for the Cauchy principal part.

Then, performing the substitution of the expression of $M_2(w)$ on the above equation, we have

$$\begin{aligned}M_1(w)=\frac{l_0^7\omega_c^5\alpha y}{4\hbar^2c_s^5}\mathrm{P}\int_0^\infty dx\frac{1}{(x-y)(x+y)}\frac{1}{x}\sum_{n,m}\Theta(E_F-\varepsilon_n)\Theta(\varepsilon_{n+m}-E_F)\\ \times\left[(m-x)^4\frac{1}{(1-e^{-(m-x)\hbar\beta\omega_c})}\frac{(e^{x\hbar\beta\omega_c}-1)}{(e^{m\hbar\beta\omega_c}-1)}\right.\\ \times C_{n,n+m}(\omega_c/c_s(m-x))\Theta(m-x)\\ -(m+x)^4\frac{1}{(1-e^{-(m+x)\hbar\beta\omega_c})}\frac{(e^{-x\hbar\beta\omega_c}-1)}{(e^{m\hbar\beta\omega_c}-1)}\\ \times C_{n,n+m}(\omega_c/c_s(m+x))\\ +(x-m)^4\frac{1}{(1-e^{-(x-m)\hbar\beta\omega_c})}\frac{(e^{-x\hbar\beta\omega_c}-1)}{(e^{-m\hbar\beta\omega_c}-1)}\\ \left.\times C_{n,n+m}(\omega_c/c_s(x-m))\Theta(x-m)\right]\ .\end{aligned} \tag{20}$$

The numerical results are obtained with the following set of values for the constants:

$$\begin{aligned}&c_s=5\times10^5\ \mathrm{cm\,s^{-1}},\quad \Xi_d=17.78\times10^{-12}\ \mathrm{erg}\ ,\\ &\rho=2.33\ \mathrm{g\,cm^{-3}},\quad d=100\ \text{Å}\ ,\\ &m_b=0.189m_e,\quad n_e=4.7\times10^{11}\ \mathrm{cm^{-2}}\ .\end{aligned} \tag{21}$$

Our numerical calculation of $M_1(w)$ clearly exhibits both the contributions from the absorption and emission phonon processes, as is seen in Fig. 1. Furthermore, the set of nonzero transitions gives rise to a very detailed structure for $M_1(w)$, which is not found in Ref. 10. In Fig. 1 we show the behavior of the real and imaginary parts of the MF, for different values of the magnetic field ($H=6.58$, 10, and 20 T) and a fixed temperature, $T=77$ K. We observe that the magnitudes of both $M_2(\omega)/\omega_c$ and $M_1(\omega)/\omega_c$, reflecting, respectively, the dissipative and reactive effects on the electron gas, decrease as the magnetic field is raised. We can also verify that the number of dips at the $M_2(\omega)$ structure increases as the calculation is performed at lower magnetic field. This is associated with the possibility of occurrence of transitions from higher filled Landau levels in so far as one gets far from the quantum limit. In our case, with $n_e=4.7\times10^{11}$ $\mathrm{cm^{-2}}$, the number of completely filled Landau levels is, respectively, $N=1,2,3$ for magnetic field intensities $H=20$, 10, and 6.58 T.

In Fig. 2 we can see, in detail, the frequency dependence and the structure relations between $M_2(w)$ and $M_1(w)$ for the case of $H=10$ T and $T=77$ K. We can observe the oscillating behavior of $M_1(\omega)$ and the resonance peaks, for both absorption and emission phonon processes, around each resonance of integer harmonics.

Figure 3 describes separately each nonzero transition contribution from the two filled initial Landau levels $n=0$ and $n=1$ ($H=10$ T), to a final state $n+m$, with $m=1,2,3$, as well as the total MF imaginary part, for a temperature $T=77$ K. It is easy to observe two principal peaks, for both phonon absorption and emission contri-

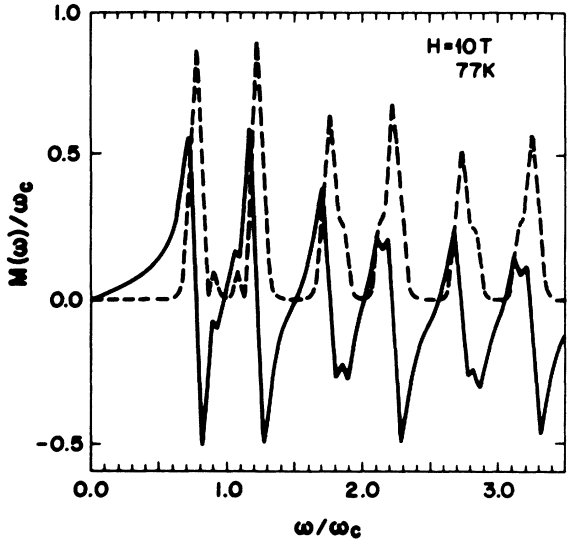

FIG. 2. Illustration of the relation between the imaginary part (dashed line) and the corresponding real part (solid line) of MF for $H=10$ T and $T=77$ K, in units of w_c. The magnitude of the phonon resonance peaks decreases as one goes to higher frequencies.

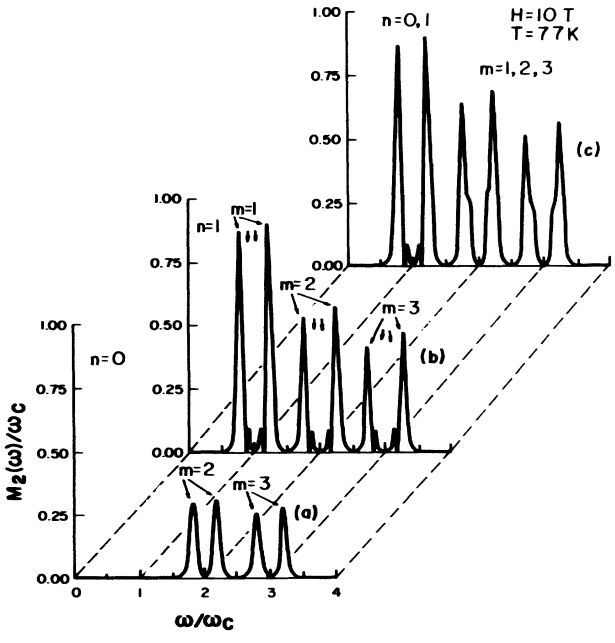

FIG. 3. The contributions to $M_2(w)$ corresponding to each specific Landau-levels transitions $(n, n+m)$. One observes (b) the appearance of split absorption and emission phonon resonance peaks for transitions from the initial state $n>0$, e.g., $n=1$ and $m=1,2,3$, in contrast with (a) the single ones for the nonzero transitions from the lowest Landau level, e.g., $n=0$ and $m=2,3$. The total MF imaginary part is exhibited in (c), in units of w_c.

butions, as well as the appearance of minor peaks strongly related to specific transitions from initial states $n>0$.

A systematic study of the temperature dependence of MF is described in Fig. 4. In general, the magnitude of the emission and absorption peaks increases as the temperature is raised. Although they have approximately the same magnitude at high temperatures, in the case of low temperatures the intensity corresponding to phonon emission becomes considerably greater than the absorption peaks, as expected.

Now we use $M_1(w)$ and $M_2(w)$ in Eqs. (12) and (13) in order to evaluate the dynamical conductivity, $\sigma(w)$. Its frequency dependence is illustrated by Fig. 5, for both phonon absorption and emission processes. Furthermore, it is shown the behavior of both real and imaginary part of $\sigma_-(w)$, as a function of the temperature and magnetic field, in units of σ_0, which is defined as

$$\sigma_0=\frac{n_e e^2}{m_b \omega_c} . \tag{22}$$

It is worthwhile to notice the occurrence of the split peaks in the conductivity for low magnetic field, in a good agreement with experimental results.[19] In our approach, this is a direct result of some Landau-level transitions and we ascribe it as the real description of the unexpected splitting of the CR line shape, in a 2D EG, as observed by Schlesinger *et al.*[19] Furthermore, we notice that the magnitude of the principal subharmonic resonance, i.e., $y=1$, clearly exhibits a linear temperature dependence at a low temperature regime. Also, their magnitude and width decrease as the magnetic field is

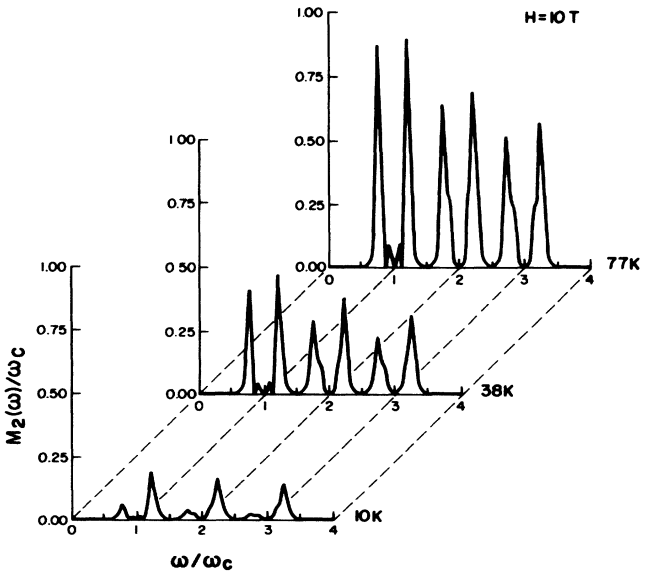

FIG. 4. The temperature behavior of $M_2(w)$, in units of w_c, for the case of $H=10$ T. At very low temperature the magnitude of the peaks corresponding to the absorption of phonons decreases more strongly than the emission ones, but the split peaks structure remains.

raised. This result, which seems to be the expected one, since it corresponds to the electron system becoming more localized, completely disagrees with the conclusion of Hu and O'Connell.[10] Finally, we want to point out that the line shape of the CR is quite insensitive to the temperature, so that the split peak remains in the whole range of temperature we have used.

IV. FINAL REMARKS

In the present work, we have investigated the role of the interaction between a two-dimensional electron gas and surface LA phonons, at the presence of a strong magnetic field. We have used the memory-function formalism in order to evaluate the temperature and the magnetic field dependence of the magnetophonon conductivity.

In our approach the broadening of the Landau levels are neglected, so that the conductivity of the system is derived only by thermal electron excitation of transitions between Landau levels. In this sense, we have taken care of some unallowed transitions, reflecting the fact that the Fermi-Dirac statistics unable the electron to make transitions to states that are already occupied. On the other

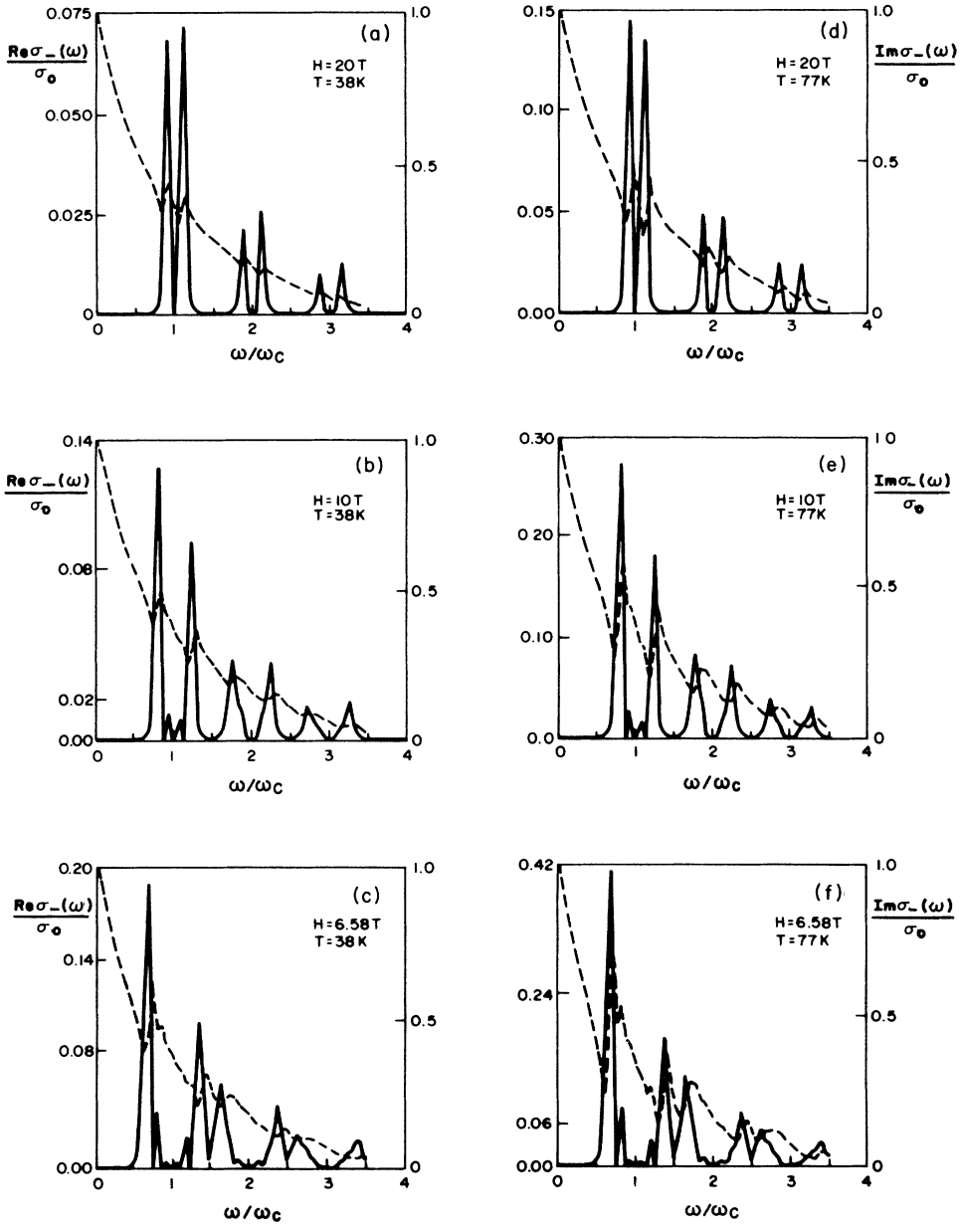

FIG. 5. The real (solid lines) and the imaginary (dashed lines) parts of the dynamical conductivity, $\sigma_{-}(w)$, in units of σ_0, for different temperatures ($T=38$ K, 77 K) and magnetic fields ($H=6.58$ T, 10 T, 20 T).

hand, we have verified in our calculation that nonzero transition contributions from initial states n ($n > 0$) give rise to n dips to the imaginary part of the MF, in addition to those which occur at the integer resonance harmonics and half-integer. In spite of that, our systematic study of cyclotron resonance properties in a 2D EG has revealed a very peculiar MF structure for both absorption and emission phonon processes. Furthermore, we have also verified that the real part of the dynamical conductivity should always exhibit a splitted resonance peak at lower magnetic fields, against the single one at the quantum limit. This interesting result derived from the Landau-level occupation and the transition contributions may provide the basis for understanding the similar experimental results obtained by Schlesinger *et al.*[19] Besides, we have noticed that the magnitude, the width, and the number of split conductivity peaks increase as the intensity of the magnetic field decreases. On the other hand, the splitting effect proved to be insensitive to the temperature, at least in the temperature range we have used.

Finally, it is worthwhile to point out that although we have performed the calculation of the cyclotron resonance to the case of a silicon MOSFET, there would be no problems in applying the model to other 2D EG materials, e.g., $Ga_{1-x}Al_xAs/GaAs$ quantum wells, as well as to a quasi-1D EG quantum wire, whose calculations are now in progress.

ACKNOWLEDGMENTS

We wish to express our sincere thanks to Dr. S. Das Sarma for stimulating discussions at the beginning of this work.

[1]T. Ando, A. B. Fowler, and F. Stern, Rev. Mod. Phys. **54**, 37 (1982); A. Gold, Z. Phys. B **63**, 1 (1986).

[2]S. Das Sarma and A. Madhukar, Phys. Rev. B **22**, 2823 (1980).

[3]Wu Xiaoguang, F. M. Peeters, and J. T. Devreese, Phys. Rev. B **36**, 9760 (1987); **36**, 9765 (1987); Phys. Status Solidi B **143**, 581 (1987).

[4]D. M. Larsen, Phys. Rev. B **30**, 4595 (1984).

[5]B. Horovitz and A. Madhukar, Solid State Commun. **32**, 695 (1978).

[6]A. Wixforth, J. P. Kotthaus, and G. Weimann, Phys. Rev. Lett. **56**, 2104 (1986).

[7]M. A. Brummell, R. J. Nicholas, M. A. Hopkins, J. J. Harris, and C. T. Foxon, Phys. Rev. Lett. **58**, 77 (1987).

[8]C. E. Leal, I. C. da Cunha Lima, A. Troper, and S. Das Sarma, Phys. Rev. B **35**, 4095 (1987).

[9]M. Degani and O. Hipólito, Superlatt. Microstruct. **5**, 141 (1989).

[10]G. Y. Hu and R. F. O'Connell, Physica A **151**, 33 (1988).

[11]W. Götze and P. Wölfle, Phys. Rev. B **6**, 1226 (1972).

[12]C. S. Ting, S. C. Ying, and J. J. Quinn, Phys. Rev. B **16**, 5394 (1977).

[13]I. C. da Cunha Lima, C. E. Leal, and A. Troper; in *Leite Lopes Festschrift: A Pioneer Physicist in the Third World*, edited by N. Fleury, S. Joffily, J. A. Martins Simoes, and A. Troper (World Scientific, Singapore, 1988), p. 191.

[14]I. C. da Cunha Lima and S. C. Ying, J. Phys. C **18**, 2887 (1985); J. Wagenhuber, K. W. Becker, and U. Rossler, Z. Phys. B **73**, 201 (1988).

[15]G. Arfken, *Mathematical Methods for Physicists* (Academic, New York, 1970).

[16]See, for example, G. D. Mahan, *Many Particle Physics* (Plenum, New York, 1981).

[17]S. Kawaji, J. Phys. Soc. Jpn. **27**, 906 (1969).

[18]T. A. Kennedy, B. D. McCombe, D. C. Tsui, and R. J. Wagner, Surf. Sci. **73**, 500 (1978).

[19]Z. Schlesinger, S. J. Allen, J. C. M. Hwang, P. M. Platzman, and N. Tzoar, Phys. Rev. B **30**, 435 (1984).